Repeated transients of weakly nonlinear traveling-wave convection

Paul Kolodner
AT&T Bell Laboratories, Murray Hill, New Jersey 07974-0636
(Received 16 July 1992; revised manuscript received 12 October 1992)

I present experimental observations of weakly nonlinear traveling-wave convection in ethanol-water mixtures in a narrow, rectangular cell of variable aspect ratio. Over ranges in aspect ratio separated by approximately unity, the first nonlinear state seen above the onset of convection consists of irregular "repeated transients," in which small-amplitude traveling waves initially grow with no change in spatial profile, then lose stability, and finally collapse back down to small amplitude. These states differ qualitatively from the "blinking" states seen just above onset at other aspect ratios, in which wave amplitude alternates regularly back and forth across the cell. The collapse in the "repeated-transient" state appears to be caused by a dephasing of the pattern which is due to the nonlinear dependence of wave number on amplitude. This dephasing shifts the pattern off resonance, causing its decay.

PACS number(s): 47.27.Te, 47.20.Ky

I. INTRODUCTION

Convection in thin, horizontal layers of binary fluid mixtures has attracted a great deal of experimental and theoretical attention in the past few years because the typical convective state observed in this system is one of traveling waves (TW's) [1]. In a narrow rectangular or annular container, the nonlinear TW states seen above the onset of convection consist of convective rolls aligned parallel to the short side of the container which propagate laterally, parallel to the long side [2].

Because of the Soret effect [3], four dimensionless numbers must be used to characterize the convective state in the binary fluid mixture: the usual Rayleigh number R (proportional to the applied temperature difference), the Prandtl number P (the ratio of the kinematic viscosity to the thermal diffusivity), the Lewis number L (the ratio of the diffusivities of solute and heat), and the separation ratio ψ, which is defined as follows:

$$\psi = -\frac{\frac{\partial \rho}{\partial c}}{\frac{\partial \rho}{\partial T}} c(1-c) S_T \ . \tag{1}$$

Here, ρ is the density, c is the solute concentration, T is the temperature, and S_T is the Soret coefficient. The separation ratio parametrizes the importance of density stratification due to the Soret effect relative to that caused by thermal expansion. For $\psi < -L^2 \sim 0$, the critical Rayleigh number for the onset of convection is suppressed above that in a pure fluid by a factor $r_{co} \sim 1-\psi$. For $\psi \lesssim -0.25$, this suppression is large, and the first state seen above onset in a narrow container consists of large-amplitude, spatially uniform convective rolls and which propagate laterally at low velocity. Recent experiments [4,5] have clarified the way in which mixing of the concentration field by the convective flow affects this propagation. Because of the convective mixing, such "strongly nonlinear" TW states cannot be well described by a theoretical model such as the Ginzburg-Landau (GL) equation [6], which assumes that the convective flow is a weak perturbation of the quiescent state seen just below onset. For this reason, a quantitative theoretical accounting of the experimental work in Refs. [4,5] has required numerical integration of the full Navier-Stokes equations [7].

In the present work, I discuss a different regime of nonlinear TW convection. For $-0.1 \lesssim \psi \lesssim -0.01$, the convective mixing of the concentration field is found to be weak in a narrow range of Rayleigh numbers just above onset. Because of this, my collaborators and I have referred to this regime as "weakly nonlinear" [8]. In this regime, the first nonlinear state seen above onset consists not of spatially uniform, slow TW's but of fast TW's whose amplitudes vary in space and time [8,9]. In a narrow, rectangular container, both the linear TW's seen exactly at onset and the nonlinear states triggered above onset are quasi-one-dimensional, consisting of superpositions of TW's which travel in the two directions parallel to the long side of the cell ("left" and "right"). The typical behavior seen just above onset consists of a modulated state in which TW amplitude appears alternately in the left- and right-going components. This causes the TW to "blink" back and forth between the two ends of the cell, with a period that diverges as the Rayleigh number is increased [8–10]. Because the effect of the flow on the diffusive concentration profile is weak in this regime, the perturbative approach inherent in the GL model is justified, and such a model does an excellent job of reproducing the sequence of dynamical TW states seen near onset in these experiments [11]. A marginal-stability analysis of the GL model, including complex linear coefficients [10], also gives an excellent accounting of the modulation period in the blinking state.

In a rectangular convection cell of moderate length, the physics of weakly nonlinear TW states is dominated by the principal ingredients of the model of Ref. [11]: convective growth of TW's, reflections from the ends of the cell, and nonlinear competition between oppositely propagating TW's. An important aspect of this model is

that, for simplicity, it uses *real* coefficients and zero-phase-shift end-wall reflections, so that the TW amplitude fields are also real, exhibiting only a discrete phase corresponding to the two propagation directions. As will be shown below, the nonlinear evolution of the phase field has a crucial effect on the dynamics of experimental TW patterns in this regime, and such effects are not included in this model. In particular, this model also neglects nonlinear disperison [12,13], but this effect does not seem to be an important part of the physics of regular blinking states seen in moderately long rectangular cells. Apparently, end-wall reflections cause a damping which overcomes the focusing effects of nonlinear dispersion. In an annular geometry, because there are no reflections, and because unidirectional states can be created, nonlinear dispersion dominates the dynamics [13]. This causes weakly nonlinear TW states in an annulus to be erratic at onset and to have a character which is quite unlike the first states seen in a rectangle [13]. However, this behavior is still at least qualitatively understandable in the context of a GL model with complex coefficients [12–14]. Nonlinear dispersion may also play a role in weakly nonlinear convection in very long rectangles [15], where end-wall reflections have a weaker relative effect than in short cells.

Despite the success of the GL model in explaining important aspects of experimental observations in the weakly nonlinear regime, there is one facet of the results reported in Ref. [8] which have not been explained on this basis: the effects of small changes in the cell length. In Ref. [8], we found that the first weakly nonlinear state seen above onset depends quite sensitively on Γ_x, the ratio of the cell length to its height. Changing Γ_x by only 0.25 (typically, $\Gamma_x \sim 17$ in those experiments) sufficed to drastically change the character of the first nonlinear TW state. The sequence of states seen near onset as Γ_x was changed was observed to be approximately periodic in Γ_x. Pure blinking states were seen only in rather narrow ranges of Γ_x separated by unity. At most aspect ratios, the TW state seen just above onset was what we called a "repeated transient." In this state, the overall TW amplitude grew up slowly with no modulation, appeared to saturate briefly, and then abruptly decayed. This cycle then repeated irregularly. The experiments in Ref. [8] were performed in a rather wide cell (transverse aspect ratio $\Gamma_y = 4.90$), and we found that the TW pattern exhibited structure in the transverse dimension during the high-amplitude part of the repeated-transient state. Repeated transients were seen only in a narrow range of Rayleigh numbers above onset. Above this range, regular blinking behavior was recovered.

The fact that repeated-transient states occur with unit period in Γ_x is a clear sign that resonance effects are playing a role. Like any other system of TW in a reflecting cavity, TW convection exhibits quantized resonant modes. Modulation due to beating between adjacent modes has been studied in detail in this system in the linear regime [16]. I suggest below that resonance effects are also crucial in the destabilization of the repeated-transient state in the nonlinear regime. These effects, of course, depend on the phase of the TW field in the convection cell, and this aspect of the flow cannot be explained by a GL model with real coefficients. The solutions of a GL equation with complex coefficients and complex end wall reflections could in principle exhibit a sensitive dependence on aspect ratio. This would be the minimum extension of the model in Ref. [11] that could explain the experimental results. It may also be necessary to explicitly take account of the fast spatial variations of the TW phase. These small spatial scales are averaged away in the derivation of the GL equation.

In order to stimulate theoretical work in this direction, I present further observations of repeated-transient states in this paper. The experiments of Ref. [8] have been repeated in a narrower convection cell ($\Gamma_y = 3.00$), in which the TW states are purely one dimensional. I continue to observe repeated-transient states in ranges of Γ_x separated by approximately unity. The nature of these states is explored in detail as a function of cell length and Rayleigh number, using shadowgraphic flow visualization and image-processing techniques. I conclude that repeated-transient behavior is the natural weakly nonlinear evolution of single-mode linear TW's in this system. The key to the physics of this state appears to lie in the nonlinear dependence of the wave number on the TW amplitude. Because of this dependence, the growth of the TW amplitude shifts the pattern out of resonance, and destructive interference, signaled by spatiotemporal defects, causes the collapse of the pattern. Blinking states, by contrast, represent a special case in which the oscillations of the phase of oppositely propagating TW components exactly cancel, leaving the system continually in resonance.

II. APPARATUS

The experimental apparatus and procedures used in this work have been described previously [8,16,17], so I only give a brief review here. The convection cell consists of a thin frame of ULTEM polyetherimide plastic which is clamped between a rhodium-plated, mirror-polished, electrically heated copper bottom plate and a water-cooled, transparent, sapphire top plate. The experimental fluid fills a rectangular slot in the plastic frame; one end-wall of the slot is a leaky, movable plug, which allows the length of the cell to be continuously varied under computer control. I used two different plastic frames in the course of this work, both with thickness $d = 0.35$ cm. The first, used in the work described in Ref. [8], had width $\Gamma_y = 4.90$, and the other had width $\Gamma_y = 3.00$. The cell length Γ_x can be set with a resolution of about 0.002. I concentrate in this paper on cell lengths Γ_x in the range 15–21.

The temperature difference applied vertically across the cell is typically about 2.8 K at onset and is held constant with a fractional stability of $\lesssim \pm 7 \times 10^{-5}$ by a computer-controlled ac bridge-servo system. Rayleigh numbers are quoted in this paper in terms of fractional distance ϵ above the measured onset of convection. The fluid was a 0.3-wt. % ethanol-water solution, with separation ratio $\psi = -0.021$, Prandtl number 6.97, and Lewis number 0.0077 [18]. The time scale in the experiment is

set by the vertical thermal-diffusion time, $\tau_v = 84.3$ sec. I also observed repeated-transient states at $\psi = -0.013$ and -0.043, but these results will not be described in this paper. Some additional supporting observations, such as that in Fig. 1 below, were made using cells of different sizes and fluids with different separation ratios.

The flow patterns are viewed from above by a shadowgraphic flow-visualization system. This optical system, and the complex-demodulation techniques which are used to analyze the data obtained from it, have been described in detail in Ref. [17]. The flow patterns exhibit nontrivial structure only in one spatial dimension in the narrow cell, along the axis designated x. The complex-demodulation and distortion-correction techniques described in Ref. [17] allow the profiles of the left- and right-going TW amplitudes $A_{L,R}(x,t)$ and wave numbers $k_{L,R}(x,t)$ to be extracted from sequences of shadowgraph images. Often, it is useful to integrate these quantities over the cell length, to obtain spatially averaged wave amplitudes and wave numbers, as in Figs. 6–8 below. I also record the light intensity integrated over a stripe perpendicular to the x direction, a few wavelengths away from one end of the cell, using a photomultiplier tube.

III. RESULTS

The weakly nonlinear states described in this paper exhibit spatiotemporal structures which have much in common with that exhibited by the linear TW's seen exactly at onset. Thus, although these linear TW's have already been described in some detail [16,17,19], it is useful for the purposes of orientation to repeat some of this description before proceeding.

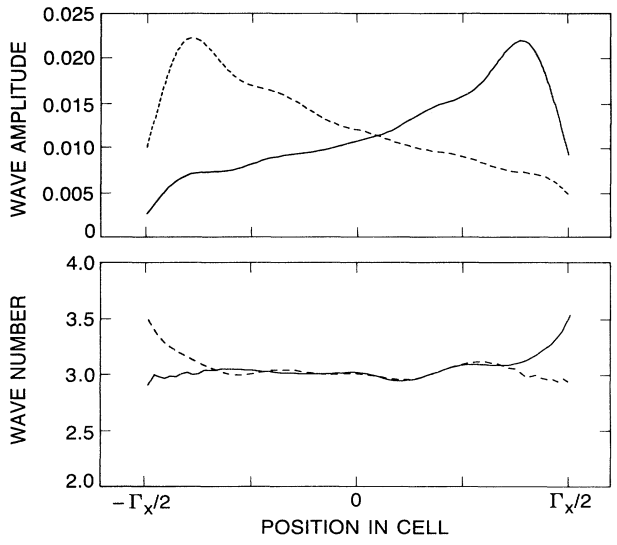

FIG. 1. Time-averaged spatial profiles of the left-TW (dashed) and right-TW (solid) amplitudes (top) and wave numbers (bottom) are shown for neutrally stable, linear TW's seen exactly at onset, using a fluid with $\psi = -0.239$ in a rectangular cell of dimensions $1 \times 4.01 \times 20.51$. In this system, the initial linear onset transient consists of a superposition of oppositely propagating TW's which grow in their direction of propagation, leading to approximately exponential spatial amplitude profiles. Except for boundary regions near the ends of the cell, the wave-number profiles are approximately constant in space.

If the Rayleigh number is increased from below to above the threshold for the onset of convection, small-amplitude TW's are amplified from the noise. These linear TW's grow in amplitude as they propagate through the system, acquiring an approximately exponential spatial amplitude profile. They also reflect with loss from the end walls of the container [17,19,20]. If, after the TW amplitude has grown to some small but nonzero level, the Rayleigh number is reduced back to the threshold value $\epsilon \equiv 0$, then the temporal growth ceases, and the transient evolves into the time-independent *neutrally stable* state illustrated in Fig. 1 for almost all aspect ratios Γ_x. In this state, the left- and right-TW amplitudes exhibit roughly exponential spatial profiles which result from the combination of propagation and temporal growth. A healing region near the end walls is caused by the reflection of the TW there [11,17,20]. The wave-number profiles also exhibit strong gradients near the end walls but are flat and equal near the center of the cell.

The linear TW state in Fig. 1 is a transient whose growth rate has been reduced to zero by setting the Rayleigh number exactly equal to the threshold for linear growth. If the Rayleigh number is now increased above this threshold, this linear transient will evolve into a weakly nonlinear state. In general, the instantaneous amplitude and wave-number profiles observed in weakly nonlinear states are similar to the linear profiles shown in Fig. 1; in particular, roughly exponential spatial amplitude profiles are common (see for example, the blinking-state amplitude profiles in Refs. [8,17] or the repeated-transient-state profiles in Fig. 9 below). However, unlike the case of the neutrally stable linear state of Fig. 1, the wave-number and amplitude profiles seen in weakly nonlinear states exhibit strong time dependences. It is the sensitive dependence of this nonlinear spatiotemporal behavior on the aspect ratio Γ_x that is the subject of this paper.

As seen in Fig. 2, this aspect-ratio dependence is exhibited by the first weakly nonlinear state seen above onset. Here, I plot the image intensity at one point in the cell as a function of time for many different aspect ratios. All of these time series were acquired in the $\Gamma_y = 3.00$ cell, at the same distance above onset: $\epsilon = 3 \times 10^{-4}$. The data are arranged by writing the aspect ratio Γ_x as the sum of an integer part n and a fractional part $\delta\Gamma = \Gamma_x - n$. The three different frames contain data for different values of n, and the vertical position of each time series represents the value of $\delta\Gamma$. Arranged in this manner, the data clearly show an approximately periodic dependence on Γ_x, with period unity. Pure blinking states, which are characterized by a regular, strong modulation of image intensity, are seen only in narrow bands of aspect ratios centered at $\delta\Gamma = 0.63$. Repeated transients, recognized by a smooth, slow increase in image intensity, followed by a saturated period, and then a sudden collapse, are the first nonlinear TW state seen for $\delta\Gamma \sim 0.13$. In between these values, the dynamics exhibit features of both kinds of state, with the repeated-transient character actually dominating for most values of Γ_x. In line with the trend

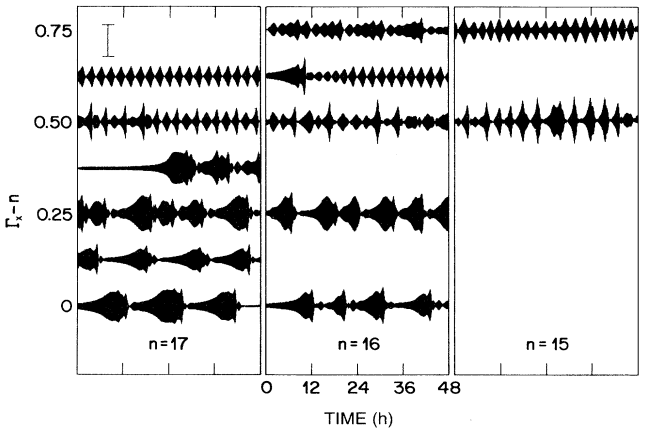

FIG. 2. The image intensity measured at a single spatial point in the $\Gamma_y=3.00$ cell is plotted as a function of time for $\epsilon=3\times10^{-4}$ for several different cell lengths Γ_x. The three frames contain data for which the integer part n of Γ_x is different, while the vertical axis shows the fractional part $\delta\Gamma=\Gamma_x-n$. Thus, for example, the bottom-left time series is for $\Gamma_x=17.00$, while the top-right time series is for $\Gamma_x=15.75$. Pure blinking states, which exhibit regular modulations in image intensity, are seen only in a narrow range of $\delta\Gamma$ centered around $\delta\Gamma=0.63$. At most other aspect ratios, the state has more of a repeated-transient character.

shown in Fig. 2, the first state seen above onset at $\Gamma_x=20.79$ was also a blinking state—see Fig. 10(b) below.

The behavior shown in Fig. 2 is representative for cells of moderate length. The authors of Ref. [15] observe more complex dynamics near onset for very long cells: $\Gamma_x\sim45$. At $\Gamma_x\sim10$ and $\Gamma_y=4.90$, as reported in Ref. [8], the first state above onset also depends sensitively on Γ_x, but the distinction between states seen at $\Gamma_x=9.75$ and 10.00 cannot be characterized as clearly as that seen in Fig. 2. The aspect-ratio dependence shown in Fig. 2 is also observed in the $\Gamma_y=4.90$ cell. However, the values of $\delta\Gamma$ at which the different states are seen depends on the cell width. For $\Gamma_y=3.00$, blinking states are seen at $\delta\Gamma=0.63$, while for $\Gamma_y=4.90$ blinking states are seen at $\delta\Gamma=0.25$ (see Fig. 7 of Ref. [8]). This dependence on cell width is discussed in greater detail in Sec. IV below. In contrast to the repeated-transient states reported for $\Gamma_y=4.90$ in Ref. [8], the flow patterns are truly one dimensional for $\Gamma_y=3.00$. The two-dimensional structure seen in the wider cell, characterized as a "tearing" of the convective pattern in Ref. [8], is not seen in these one-dimensional patterns and thus appears to be irrelevant to the physics of the repeated-transient state.

It is important to note that pure blinking states are observed at values of Γ_x in both cells at which the linear TW's seen exactly at onset exhibit strong, persistent modulation due to the interference between adjacent resonant modes [16]. At the aspect ratios at which repeated-transient states are observed, this linear modulation is only observed, if at all, as a rapidly decaying transient at onset. Apparently, despite the quantitative differences in the behavior caused by the width of the cell, the resonance condition which determines the wave number of linear TW's also plays an important role in the evolution of the weakly nonlinear state. We will see below that this is the key to the difference between blinking states and repeated transients.

Repeated-transient states are only observed in a narrow range of Rayleigh number. This is illustrated in Fig. 3, where time series of image intensity are shown for different values of ϵ in a cell of size 4.90×16.75. As shown by the curves labeled (a) and (b), the first state above onset is a repeated transient. Curve (b) shows that the repeat time in this state can be variable—this is discussed below. Pure repeated-transient states are seen for $\epsilon\lesssim0.0010$. As shown in curves (c) and (d), the signal starts to acquire the character of a blinking state as the Rayleigh number is increased above $\epsilon\sim0.0015$. At higher ϵ [curves (e) and (f)], blinking states of increasing modulation period are observed, as documented in Refs. [8–10].

Figures 4 and 5 show the dependence on ϵ of the modulation times $\tau_{\rm mod}$ of the weakly nonlinear states observed in the $\Gamma_y=4.90$ cell for $\Gamma_x=16.75$ and 16.25, respectively. For blinking states, $\tau_{\rm mod}$ is just the modulation period, while, for repeated-transient states, $\tau_{\rm mod}$ represents the average time between the sudden decreases in amplitude that mark the end of each "repeated transient." $\tau_{\rm mod}$ is normalized by the oscillation period τ_0 of the linear TW's seen exactly at onset. The time-series data in Fig. 3 are represented as some of the data points in Fig. 4. The repeated-transient states observed below

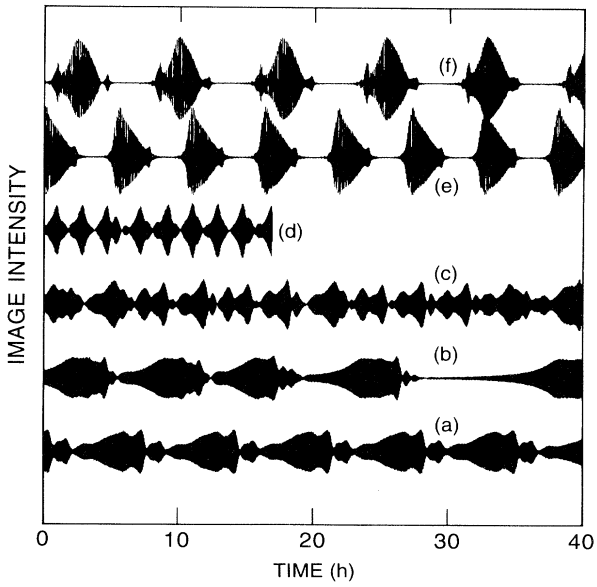

FIG. 3. The image intensity measured at a single spatial point in a cell of dimensions 4.90×16.75 is plotted as a function of time for different values of the Rayleigh number: (a) $\epsilon=0.0006$; (b) $\epsilon=0.0008$; (c) $\epsilon=0.0015$; (d) $\epsilon=0.0030$; (e) $\epsilon=0.0105$; (f) $\epsilon=0.0111$. The repeated-transient states seen at the lowest values of ϵ [(a), (b)] give way at higher ϵ to blinking states [(c), (d)] whose period grows quite long at the highest values of ϵ shown [(e), (f)] and diverges at $\epsilon\sim0.012$.

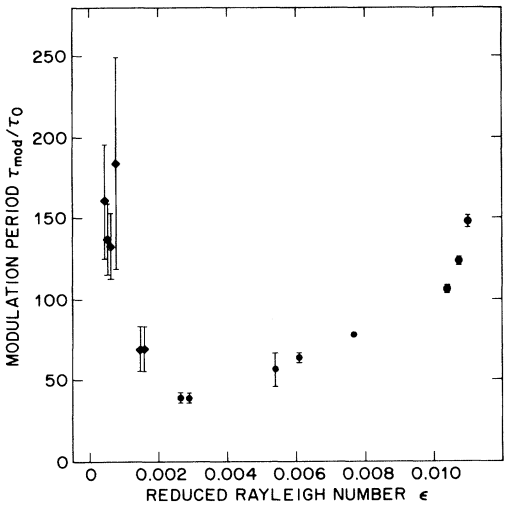

FIG. 4. The modulation period of the weakly nonlinear states observed in a cell of dimensions 4.90×16.75, normalized by the oscillation period of the linear state seen at onset, is plotted as a function of the distance ϵ above onset. The circles represent blinking states, and the diamonds represent repeated-transient states. Repeated transients are seen only at low values of ϵ, and their modulation period diverges as ϵ is reduced to zero. The modulation period of the blinking states seen at higher ϵ diverges as ϵ is increased. The error bars in this graph and Fig. 5 represent states in which the modulation period varied in time.

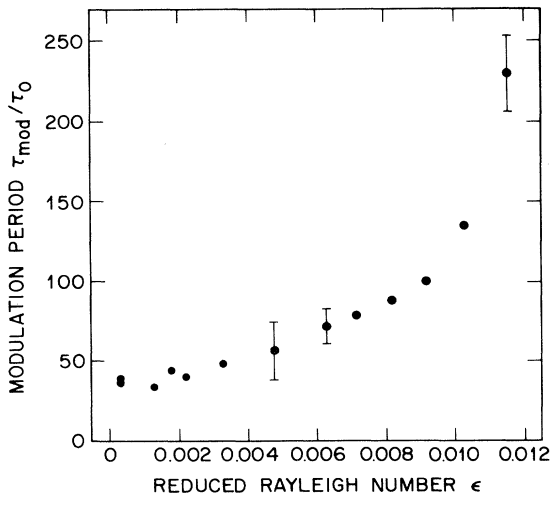

FIG. 5. The normalized modulation period of the blinking states observed in a cell of dimensions 4.90×16.25 is plotted as a function of ϵ, as in Fig. 4. At this aspect ratio, only blinking states are observed. Their modulation period diverges as ϵ increases, as in Fig. 4.

$\epsilon\sim0.002$ at $\Gamma_x=16.75$ are shown as the diamonds in Fig. 4. These modulation periods are quite variable from transient to transient, as shown by the error bars, and they appear to diverge as ϵ is reduced to zero. It is worth noting that this variability is far in excess of what would be caused by the measured temporal fluctuations in ϵ,

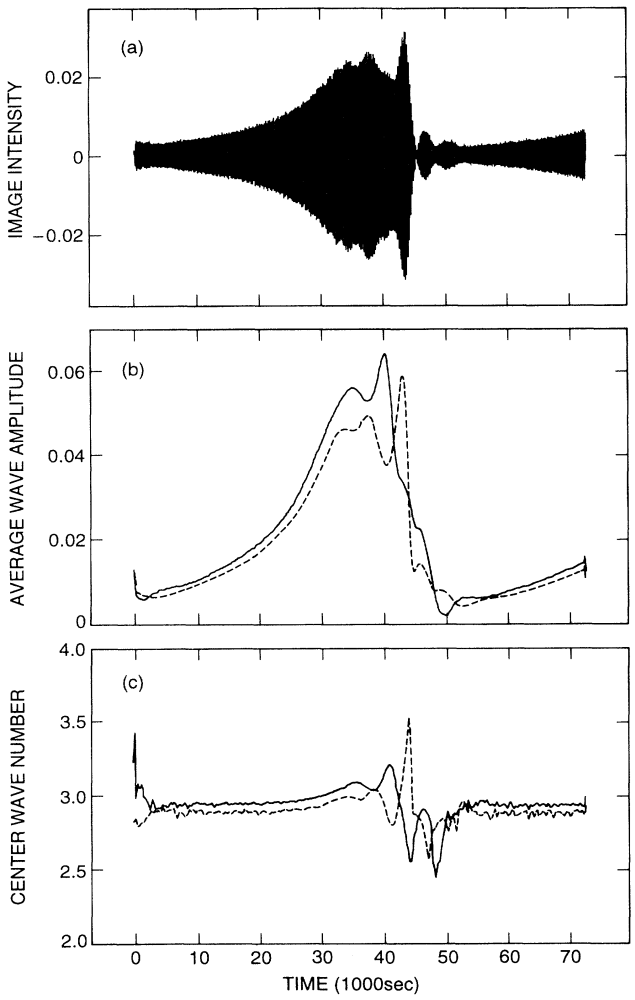

FIG. 6. Evolution of the TW pattern in one cycle of a repeated-transient state observed at $\epsilon=5\times10^{-4}$ in a cell of dimensions 3.00×17.10. (a) Time series of the image intensity measured at a single spatial point near the left edge of the cell. Smooth growth followed by modulations and sudden decay are observed. (b) The spatially averaged left- and right-TW amplitudes, as computed from complex demodulation of the shadowgraph data, are shown as the dashed and solid curves respectively. Initially, both components grow smoothly. They then begin to oscillate out of phase and then decay. As discussed in Ref. [17], the initial slight difference between the two wave amplitudes may be caused by a small asymmetry in the experimental cell. (c) The wave numbers of the left- (dashed) and right- (solid) TW components, as measured in the center of the cell, are shown as functions of time. Initially, both wave numbers are constant. They then increase slightly and oscillate out of phase as the amplitudes grow, go unstable, and decay. The loss of one wavelength in the left-TW component is seen as an abrupt drop at time $t=44\,000$ sec.

even given the strong dependence of τ_{mod} on ϵ at the lowest values in the graph. Because of this variability, it is not possible to deduce the functional dependence of τ_{mod} on ϵ, but these data are not inconsistent with an ϵ^{-1} dependence.

Above $\epsilon \sim 0.002$, the repeated-transient states give way to pure blinking states at $\Gamma_x = 16.75$, as shown by the circles in Fig. 4. The modulation period in this state diverges as ϵ is increased to about 0.012, leading to a stable confined state [8–10,21]. This behavior matches that seen for $\Gamma_x = 16.25$, where blinking states are seen all the way down to onset (Fig. 5). This divergence has been explained using the marginal-stability hypothesis in Ref. [10]; indeed, the data in Fig. 5 appear in Fig. 1(b) of that work.

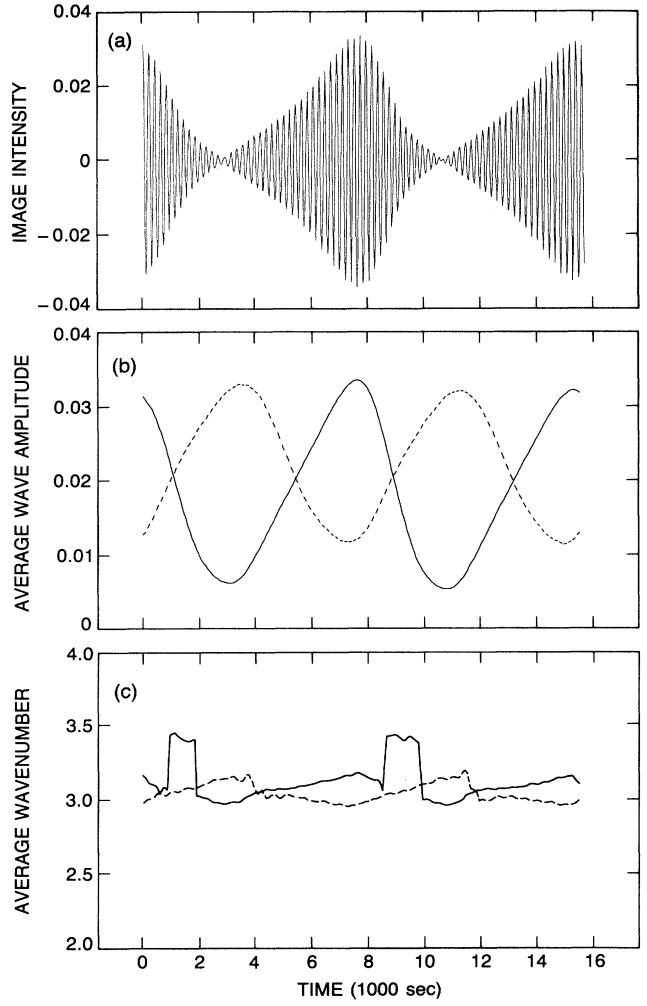

FIG. 7. Evolution of the TW pattern in two cycles of a blinking state observed at $\epsilon = 3 \times 10^{-4}$ in a cell of dimensions 3.00×17.63. (a) Time series of the image intensity measured at a single spatial point near the right edge of the cell. A smooth, complete modulation of the signal is observed. (b) Temporal evolution of the spatially averaged left- and right-TW amplitudes. The modulations in the time series in (a) correspond to an oscillation of the wave amplitude back and forth between the two TW components. (c) The spatially averaged wave numbers of the left- and right-TW components are shown as functions of time. Both wave numbers oscillate weakly in phase with the amplitude modulation. The right-TW component gains and then loses one spatial wavelength once per modulation cycle. The total round-trip phase remains constant, modulo 2π, during this run.

Figures 6 and 7 illustrate the detailed differences between the flow patterns in the repeated-transient and blinking states. Figure 6(a) shows the single-point image-intensity time series for a single cycle of a repeated-transient state observed in the $\Gamma_y = 3.00$ cell at $\epsilon = 5 \times 10^{-4}$. The characteristic slow growth, near saturation, destabilization, and collapse are plainly seen in this graph. These features are also evident in Fig. 6(b), in which the spatially averaged left- and right-wave amplitudes are plotted as functions of time. During the initial growth of this transient ($t \lesssim 30\,000$ sec), the ratio of the two wave amplitudes is constant. The pattern in this phase is the same single-mode, counterpropagating TW pattern seen in the linear state exactly at onset [17,19], and the duration of this smoothly growing phase is inversely proportional to ϵ. Above a certain amplitude, however, the amplitudes of the left- and right-TW's begin to oscillate out of phase with each other, with a period of about 5000 sec. As in the blinking state, the likely dominant cause of this oscillation is the stabilizing nonlinear interaction between the two TW components. After this oscillatory phase, whose duration is variable from transient to transient, the flow pattern decays abruptly, and the growth starts again.

Figure 6(c) shows the time evolution of the left and right wave numbers measured in the center of the cell during this run. At the low initial wave amplitudes, the two wave numbers exhibit spatial profiles similar to those seen in Fig. 1, are approximately constant in time, and have values in the center of the cell of approximately 2.90. As the TW amplitudes increase, the wave-number profiles begin to grow nonuniform, with high-amplitude regions exhibiting higher local wave numbers. This evolution causes the center wave numbers plotted in Fig. 6(c) to increase. This behavior is apparently caused by a nonlinear dependence of wave number on amplitude and is clearly seen in the blinking state in Fig. 7(c) as well. Then, coincident with the onset of the oscillations of the TW amplitudes (time $t \sim 35\,000$ sec), the local wave numbers also begin to oscillate, although these oscillations are found to cancel out when the total round-trip phase of the TW is calculated. Note in Fig. 6(c) that the left wave number, shown as the dashed curve, exhibits a sharp drop at $t = 44\,000$ sec. The amount of this sudden decrease is equal to the wave-number difference Δk between two adjacent resonant modes in this cell. This wave-number drop corresponds to a spatiotemporal defect in which one pattern wavelength in only the left-TW component is abruptly lost. The right-TW component also exhibits several spatiotemporal defects during this run, but the right-TW defects happen to occur far from the center of the cell and are thus not seen in Fig. 6(c). Spatiotemporal defects are also seen in the individual TW components in blinking states—see Ref. [17] and Fig. 7(c).

I believe that the behavior of the wave-number profiles contains the key to the physics of the repeated-transient state and the difference between this state and the blinking state. The wave number increase seen in Fig. 6(c) is numerically small, but it is not negligible compared to the wave-number difference Δk between adjacent modes. Of course, it is the *round-trip phase* of the TW which determines the stability of the system against destructive interference, not the local wave numbers. The round-trip phase in this run was carefully calculated using the full demodulated wave-number profiles and found to increase by 0.4 rad during the growing-amplitude part of this run. Thus, because of the nonlinear dependence of the wave number on the TW amplitude, the growth of the amplitudes shifts the pattern out of resonance, and this appears to cause destructive interference that is responsible for the ultimate decay of the state.

The exact history of the pattern during its dephasing and decay is highly variable from transient to transient, and this suggests why the modulation period in the repeated-transient state is so erratic. This can be clearly seen in curve (b) of Fig. 3. The fourth collapse in this sequence brought the signal to much lower amplitude than the previous three transients (compare the amplitudes at times 20 and 30 h). Thus, the system took much longer after that episode to grow back up to a nonlinear amplitude, even though the growth rate at small amplitudes is the same throughout the run.

Because the stability of the TW pattern is so sensitive to dephasing, it makes intuitive sense that the destabilization and collapse that are the signatures of the repeated-transient state should be seen at almost all aspect ratios. However, the experiments show that, if the aspect ratio is tuned exactly right, the system can find a state just above onset in which the dephasings of the opposite TW components exactly cancel, so that the total round-trip phase is constant, and the system remains in resonance. This is the blinking state. Figure 7 shows the temporal evolution of this state. As seen in Figs. 7(a) and 7(b), the TW amplitudes oscillate regularly, with a period of 8000 sec—comparable to the oscillation period in the high-amplitude phase of the repeated-transient state. As documented in Refs. [8,9,17], the alternation of TW amplitude between the two components seen in Fig. 7(b) corresponds to a "blinking" of the pattern back and forth across the experimental cell.

Figure 7(c) shows that the spatially-averaged wave numbers also oscillate in the blinking state. As in the repeated-transient state, higher wave numbers coincide with higher amplitudes in this state. Observe that the sum of the spatially averaged left- and right-TW wave numbers, which is proportional to the round-trip phase of the pattern, remains constant during the run, except for phase jumps of 2π caused by spatiotemporal defects, which appear as regular pulses in the right-wave-number signal. These defects do not affect the round-trip phase of the pattern, modulo 2π. Thus, despite the nonlinear dependence of wave number on TW amplitude, the blinking state remains continually in resonance and is thus stable.

While the nonlinear dependence of the wave number on the TW amplitude seems to play an important role in the physics of the repeated-transient state, the nonlinear competition between the left- and right-TW amplitudes that is assumed in the model of Ref. [11] is still an important effect. I believe that the similarity of the oscillation periods in the blinking and repeated-transient states—8000 and 5000 sec, respectively— is a sign of this.

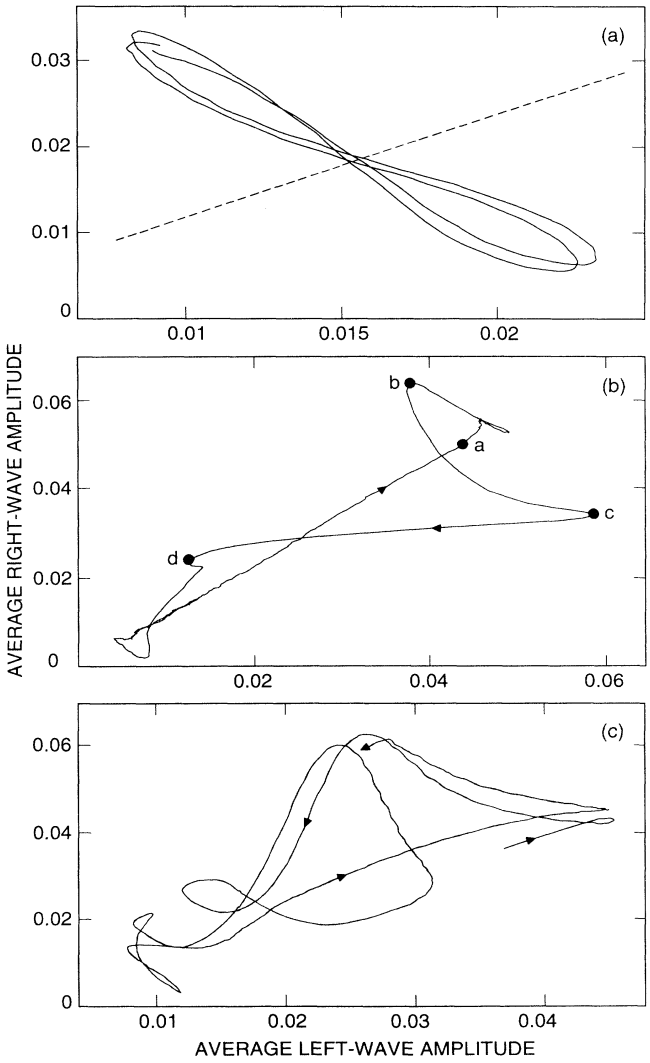

FIG. 8. Lissajous plots of the spatially averaged TW amplitudes for three weakly nonlinear states. (a) The blinking state of Fig. 7, with $\Gamma_x = 17.63$ and $\epsilon = 3 \times 10^{-4}$. The curve forms a figure 8, representing a nearly periodic repulsion from the dashed equal-amplitude line. (b) The repeated-transient state of Fig. 6, with $\Gamma_x = 17.10$ and $\epsilon = 5 \times 10^{-4}$. The arrowheads show the direction of time. The state initially grows up along the equal-amplitude line and is then repelled from it, decaying back down to small amplitude, while oscillating back and forth across the line. (c) An irregular repeated-transient state, with $\Gamma_x = 17.24$ and $\epsilon = 7 \times 10^{-4}$. The first collapse is interrupted by a sudden amplitude burst and decay, accompanied by crossings of the equal-amplitude line. The growth and repulsion from the line then start again.

Another way of highlighting this competition is to plot the spatially averaged left- and right-TW amplitudes against one another, making a Lissajous pattern, as was done in Ref. [17]. This is shown for three different weakly nonlinear states in Fig. 8. Figure 8(a), taken from Ref. [17], shows the plot for the blinking state of Fig. 7. The curve exhibits nearly periodic oscillations in the form of a figure 8, representing a regular exchange of wave amplitude between the left- and right-TW components. This figure-8 shape was also observed in numerical integrations of a generalized GL model in Ref. [22]. The curve in Fig. 8(a) appears to be repelled from the equal-amplitude line [dashed line in Fig. 8(a)]. As pointed out in Ref. [17], this repulsion is a sign of the nonlinear competition between the two TW components and is a hallmark of all weakly nonlinear TW states.

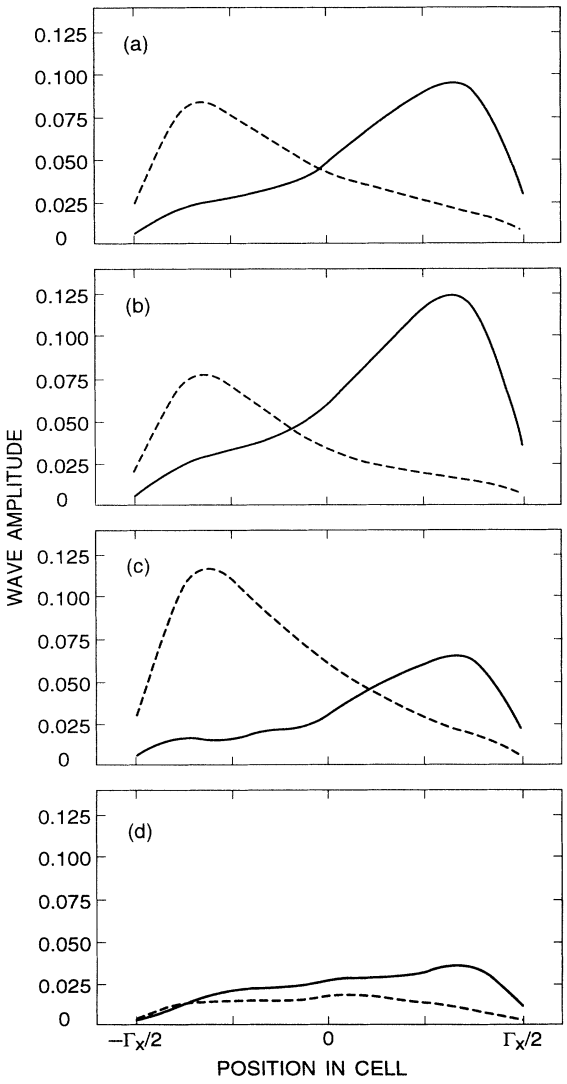

FIG. 9. The spatial profiles of the left-TW (dashed) and right-TW (solid) amplitudes are shown for the points marked a–d in Fig. 8(b). The decay of this repeated-transient state is accompanied by the exchange of wave amplitude back and forth between the two TW components.

Figure 8(b) shows the repeated-transient state of Fig. 6 in the same representation. Here, the arrowheads indicate the direction of increasing time. Initially (before the point labeled a), the state moves out along the equal-amplitude line, presenting a pattern of counterpropagating, linear TW's which grows up with no change in spatial structure. Above a certain amplitude, however, the pattern loses stability, and the curve is repelled from the equal-amplitude line [moving to point b Fig. 8(b)]. The collapse of the repeated-transient state is accompanied by an exchange of amplitude between the two TW components, as represented by the oscillations of the curve back and forth across the equal-amplitude line, between the points labeled b,c, and d. This can also be seen directly in the spatial profiles of the left- and right-TW amplitudes. The amplitude profiles corresponding to the labeled points in Fig. 8 are shown in Fig. 9.

The irregular modulation period observed in the repeated-transient state was associated above with a sensitive dependence of the stability of the TW pattern on the round-trip phase. As shown in Fig. 8(c), this is reflected in erratic dynamics during the collapse of the TW pattern. In this run, the amplitudes initially grow up along the equal-amplitude line and then collapse, as in

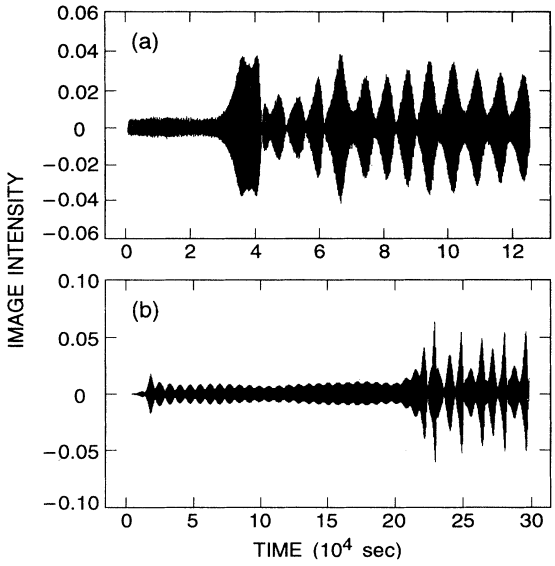

FIG. 10. The time evolution of the image intensity measured at a single spatial point is shown for two experiments in which linear TW's evolved into blinking states. (a) $\Gamma_x = 15.75$. In this run, the linear state was held exactly at onset for such a long time that all linear modes but one decayed to zero amplitude. The increase in ϵ to 3×10^{-4} at time $t = 28\,000$ sec was followed by growth, saturation, oscillations, and abrupt decay, exactly as in a repeated-transient state. The system then evolved into a blinking state. (b) $\Gamma_x = 20.79$. As can be seen at the beginning of the graph, this run began with strong modulation due to the interference between adjacent linear TW modes. The system was held at onset until $t = 200\,000$ sec, which was not long enough for the weaker linear mode to decay completely. The subsequent increase in ϵ to 3×10^{-4} resulted in an almost direct transition to the blinking state.

Fig. 8(b). Here, however, the curve makes an additional oscillation across the line, accompanied by a burst in amplitude, before finally decaying to small amplitude and slowly growing back up again.

Figure 10 shows a final observation concerning the initial evolution of linear TW into weakly nonlinear states upon increasing the Rayleigh number just above onset. As can be seen in the final state in the two parts of the figure, both experiments were performed at aspect ratios for which blinking states are the first nonlinear state above onset. The difference between these two experiments is that the run in Fig. 10(a) was begun by waiting a very long time at small amplitude near onset, so that all linear modes except one had decayed away before the nonlinear state was created. The system was also held at onset very long time in Fig. 10(b), but not long enough for the beats between adjacent linear modes to decay completely. Figure 10(a) shows that, even at an aspect ratio for which the final state is a regular blinking state, the natural nonlinear evolution of a single linear mode is one cycle of the repeated-transient state. After the first collapse of this state at time $t=40\,000$ sec, the system evolves into blinking (the same evolution can be seen for $\Gamma_x=16.63$ in Fig. 2). By contrast, in Fig. 10(b), when a second linear mode is present in the initial linear state—even at small amplitude—the system evolves almost directly into blinking. The initial linear state in Fig. 10(b) already exhibits blinking of the TW amplitudes, with a spatially uniform wave-number profile [16]. The only adjustment required to form the nonlinear TW pattern is for the modulation to deepen and for the TW amplitudes to grow. This in turn causes the initially uniform wave-number profiles to be modulated as in Fig. 7(c).

IV. DISCUSSION

The experiments reported in this paper show that, for small $|\psi|$, the natural evolution of single-mode, linear, counterpropagating TW's just above onset in a rectangular cell of moderate length consists of slow growth, saturation, destabilization, and collapse back to small amplitude. At most values of the aspect ratio Γ_x, this process repeats irregularly, making a "repeated-transient" state. To obtain a regular blinking state close to onset, careful tuning of the cell length is required. Above a certain threshold, this tuning is no longer necessary to get a blinking state. These are the bare experimental facts which lack a theoretical explanation.

The nonlinear evolution of the TW phase field seems to be the key physical ingredient that needs to be added to theories of weakly nonlinear TW convection to account for these observations. The initial destabilization of the intermediate saturated TW in the repeated-transient state appears to be caused by the real nonlinear competition between the left- and right-TW amplitudes. However, this alone does not cause the sudden collapse of the wave amplitude, as shown by the existence of regular blinking states in narrow ranges of Γ_x. I have presented evidence that the wave number of the pattern depends nonlinearly on the TW amplitude in both states. The dephasing of the pattern that this dependence causes at high amplitude appears to be the true cause of the abrupt collapse of the pattern in the repeated-transient state. This phase argument suggests why repeated-transient states are seen for most aspect ratios and why the repeat times in this state are so irregular.

Viewed in this context, regular blinking states are very special solutions to the equations which govern this system. Sufficiently close to onset, the precise tuning of cell length that they require is necessary for the nonlinear phase shifts in the oppositely propagating TW to cancel exactly, so that the pattern remains continually in resonance. At aspect ratios where blinking states exist close to onset, they are quite robust: Even if the system is prepared in a single linear mode, so that the first nonlinear event in a run is a transient of the type seen in repeated-transient states, the system starts to blink immediately after the first collapse in TW amplitude.

Judging from the single-spatial-point image-intensity time series in Figs. 2 and 3, repeated-transient states appear to be similar to the "dispersive chaos" seen in annular convection cells under similar experimental conditions [13]. Both states are seen just above onset and consist of slow, linear growth followed by an abrupt collapse in TW amplitude. However, this resemblance is superficial. Dispersive chaos can be observed in *unidirectional* TW states, where the nonlinear competition between oppositely propagating TW's is irrelevant, and dispersive chaos has been shown to be caused by strong nonlinear dispersion [13,14]. Repeated-transient behavior, by contrast, appears in manifestly counterpropagating states only, and I have suggested that the oscillations seen in the intermediate, nearly saturated state that precedes the abrupt collapse are evidence of real nonlinear competition between left- and right-TW amplitudes. This being said, it may still be that nonlinear dispersion is an important part of the physics of repeated-transient states, since this effect couples TW amplitude and phase. This is discussed below.

Given the importance of resonance effects and the possibility of computing spatial wave-number profiles from shadowgraph data, it is very tempting to try to draw quantitative conclusions from the data about the relationship between the observed TW wave numbers and theoretical predictions concerning linear TW's [23] and modulational instabilities [24]. For example, it would be quite useful to insert the wave numbers k_n measured in a nonlinear state into the resonance condition,

$$k_n\Gamma_x+\phi_r=n\pi \tag{2}$$

(with ϕ_r the phase shift of the TW on reflection from the end walls and n the mode number) and deduce the value of ϕ_r. One would also like to compare the wave number of a nonlinear state with the theoretically computed linear critical wave number k_e, as was done by Fineberg, Moses, and Steinberg [9]. However, this kind of undertaking is very hazardous, for several reasons. First, the wave-number profiles in both linear and weakly nonlinear TW states vary in space as well as in time, with especially strong spatial variations near the end walls [17]. Thus, the wave number k_n of the nth mode is not well defined. Because of this, the resonance condition must be rewrit-

ten in terms of a round-trip phase [or a spatially averaged wave number, as in Fig. 7(c)]. This round-trip phase is quite sensitive to small distortions and computational errors, so that even this quantity cannot be computed very accurately. (Fortunately, these errors affect the round-trip phase in the same way in the middle of the run in Fig. 6 as they do at the beginning, so that the statement that the nonlinear wave-number dependence causes a round-trip phase *shift* by 0.4 rad is fairly accurate.)

Not only is the wave number poorly defined in these states, but the linear critical wave number k_c is also very difficult to determine. k_c is quite sensitive to the width of the cell, even at $\Gamma_y=5$ [25]. Thus, calculations of k_c for $\Gamma_y=\infty$ [23] are not a useful guide in these experiments. It is for this reason that linear mode beating and blinking states just above onset are seen at such different values of $\delta\Gamma$ for the two values of Γ_y in these experiments. In addition, even the experimentally observed wave number of linear TW's may not bear a straightforward relationship to the true value of k_c. In Ref. [16], we analyzed persistent beating caused by interference of adjacent linear modes by expanding the linear part of the GL equation in powers of Γ_x^{-1}. To first order, we found that persistent beats between modes n and $n+1$ are observed when the aspect ratio is tuned to a value Γ_n for which $(k_n+k_{n+1})/2=k_c$. Since repeated-transient states are observed for $\Gamma_x\sim\Gamma_n-\frac{1}{2}$, this appears to mean that the linear wave number is close to k_c for aspect ratios at which repeated-transient states are observed. However, terms encountered at order Γ_x^{-2} in the expansion of the GL equation have the effect of introducing an extra phase shift into the formula for Γ_n, so that persistent beating between linear modes may actually be happening at aspect ratios where the linear wave number is much closer to k_c [26]. Thus, without extensive measurements of linear mode beating over a range of cell lengths, the linear critical wave number can be quite uncertain. For this reason, I have not phrased any of my interpretation of repeated transients in terms of quantitative comparisons with linear or nonlinear theories of laterally infinite TW's, and I think that any conclusions based on such comparisons are as yet unreliable.

Given that quantitative wave-number measurements are not a useful guide to the physics in this system in the sense just described, it is natural to ask whether there are any theoretical approaches which could predict the properties of repeated-transient states in a qualitative manner. There are several avenues which have been explored. Cross [11] has shown numerically that a supercritical GL model of real TW amplitudes in a finite container with real coefficients can exhibit blinking states. The sequence of blinking states seen in Ref. [11] matches the experimental observations in Refs. [8,9]. The dynamical behavior in this model is caused by advection, end wall reflections, and the nonlinear competition between oppositely propagating TW components. Because the TW fields in this model are strictly real, they cannot exhibit a spatiotemporally varying wave-number profile or any sensitivity to small changes in aspect ratio. However, both of these effects are possible if the end wall reflection coefficients are made complex, even if the coefficients in the GL equation remain real. In this case, the TW fields must also be complex, and the system acquires a round-trip phase. However, the nonlinear dependence of wave number on amplitude has not been explored in this model, and preliminary numerical work has revealed no sensitive dependence of the TW state above onset on the aspect ratio [27].

It is known that, for the fluid used in the present experiments, the nonlinear frequency-renormalization coefficient in the complex GL model of this system is very large [13,14]. It is this fact which is responsible for the observation of "dispersive chaos" in long, annular convection cells [12–14]. This coefficient is set to zero in the real-coefficient, complex-field model outlined in the previous paragraph. If this model still fails to exhibit repeated-transient solutions, an obvious next step would be to include the nonlinear frequency renormalization term, since this term couples the TW amplitude and phase.

Dangelmayr, Knobloch, and Wegelin [28] have also studied weakly nonlinear TW patterns in finite containers, this time using a multiscale expansion to produce exact, small-amplitude solutions to the complex GL equation. They also see a sequence of blinking states near onset, and they find a unit-period dependence on the aspect ratio. However, repeated-transient states have not been seen explicitly in this work.

There is another extension of the GL model which might introduce a sensitivity to cell length: the inclusion of nonadiabatic effects. Normally, the GL model is derived using a separation-of-scales analysis in which all structure on length scales comparable to or smaller than the pattern wavelength are averaged away. In a finite system, however, such structure may not average exactly to zero. Bensimon, Shraiman, and Croquette [29] have shown how such nonadiabatic effects can be introduced into the GL equation as a small perturbation, and they discussed the conditions under which this could cause pinning of fronts of TW's. It is not known, however, whether such effects would cause a sensitive dependence of dynamics on the length of a rectangular convection cell.

In summary, the key to the repeated-transient state appears to lie in the nonlinear coupling between the amplitude and phase fields. There are several ways in which this effect can be introduced into the real GL model that is often invoked to explain the dynamical states seen in these experiments. I hope that the careful measurements presented in this paper will encourage theorists to pursue these directions.

ACKNOWLEDGMENTS

The experiments described in this paper were begun in collaboration with C. M. Surko. I also thank M. C. Cross, P. C. Hohenberg, and E. Knobloch for useful discussions.

[1] R. W. Walden, P. Kolodner, A. Passner, and C. M. Surko, Phys. Lett. **55**, 496 (1985).
[2] For an illustration of the kinds of dynamical behavior that can be observed in strongly nonlinear TW convection in a narrow geometry, see D. Bensimon, P. Kolodner, C. M. Surko, H. Williams, and V. Croquette, J. Fluid Mech. **217**, 441 (1990).
[3] D. T. J. Hurle and E. Jakeman, J. Fluid Mech. **47**, 667 (1971).
[4] D. R. Ohlsen, S. Y. Yamamoto, C. M. Surko, and P. Kolodner, Phys. Rev. Lett. **65**, 1431 (1990).
[5] K. D. Eaton, D. R. Ohlsen, S. Y. Yamamoto, C. M. Surko, W. Barten, M. Lücke, M. Kamps, and P. Kolodner, Phys. Rev. A **43**, 7105 (1991); B. L. Winkler and P. Kolodner, J. Fluid Mech. **240**, 31 (1992).
[6] A. C. Newell, in *Nonlinear Wave Motion,* Lectures in Applied Mathematics, edited by A. C. Newell (American Mathematical Society, Providence, 1974), Vol. 15, p. 157.
[7] W. Barten, M. Lücke, and M. Kamps, in *Proceedings of the NATO Advanced Research Workshop on Nonlinear Evolution of Spatio-temporal Structures in Dissipative Continuous Systems,* Vol. 225 of *NATO Advanced Study Institute, Series B2: Physics,* edited by F. H. Busse and L. Kramer (Plenum, New York, 1990), p. 131.
[8] P. Kolodner and C. M. Surko, Phys. Rev. Lett. **61**, 842 (1988); P. Kolodner, C. M. Surko, and H. Williams, Physica D **37**, 319 (1989).
[9] J. Fineberg, E. Moses, and V. Steinberg, Phys. Rev. Lett. **61**, 838 (1988); V. Steinberg, J. Fineberg, E. Moses, and I. Rehberg, Physica D **37**, 359 (1989).
[10] J. Fineberg, V. Steinberg, and P. Kolodner, Phys. Rev. A **41**, 5743 (1990).
[11] M. C. Cross, Phys. Rev. A **38**, 3593 (1988); M. C. Cross, Physica D **37**, 315 (1989).
[12] C. S. Bretherton and E. A. Spiegel, Phys. Lett. A **96**, 152 (1983).
[13] P. Kolodner, J. A. Glazier, and H. L. Williams, Phys. Rev. Lett. **65**, 1579 (1990); J. A. Glazier, P. Kolodner, and H. Williams, J. Stat. Phys. **64**, 945 (1991).
[14] W. Schöpf and L. Kramer, Phys. Rev. Lett. **66**, 2316 (1991).
[15] V. Steinberg and E. Kaplan, in *Proceedings of the NATO Advanced Research Workshop on Spontaneous Formation of Space-Time Structures and Criticality,* edited by T. Riste and D. Sherrington (Kluwer, Dordrecht, 1991), p. 207.
[16] P. Kolodner, C. M. Surko, H. L. Williams, and A. Passner, in *Propagation in Systems Far from Equilibrium,* edited by J. E. Wesfreid *et al.* (Springer-Verlag, Berlin, 1988), p. 282.
[17] P. Kolodner and H. Williams, in *Proceedings of the NATO Advanced Research Workshop on Nonlinear Evolution of Spatio-temporal Structures in Dissipative Continuous Systems* (Ref. [7]), p. 73.
[18] P. Kolodner, H. Williams, and C. Moe, J. Chem. Phys. **88**, 6512 (1988).
[19] P. Kolodner, A. Passner, C. M. Surko, and R. W. Walden, Phys. Rev. Lett. **56**, 2621 (1986); C. M. Surko and P. Kolodner, *ibid.* **58**, 2055 (1987).
[20] M. S. Bourzutschky and M. C. Cross, Phys. Rev. A **45**, 8317 (1992).
[21] E. Moses, J. Fineberg, and V. Steinberg, Phys. Rev. A **35**, 2757 (1987); R. Heinrichs, G. Ahlers, and D. S. Cannell, *ibid.* **35**, 2761 (1987).
[22] M. Bestehorn, R. Friedrich, and H. Haken, Z. Phys. B **72**, 265 (1988).
[23] S. J. Linz and M. Lücke, Phys. Rev. A **35**, 3997 (1987); B. J. A. Zielinska and H. R. Brand, *ibid.* **35**, 4349 (1987); E. Knobloch and D. R. Moore, *ibid.* **37**, 860 (1988); M. C. Cross and K. Kim, *ibid.* **37**, 3909 (1988).
[24] J. P. Stuart and R. C. DiPrima, Proc. R. Soc. London, Ser. A **362**, 29 (1978); H. R. Brand and R. J. Deissler, Phys. Rev. A **45**, 3732 (1992); W. van Saarloos and P. C. Hohenberg, Physica D **56**, 303 (1992).
[25] P. Kolodner (unpublished).
[26] P. Kolodner, C. M. Surko, and M. C. Cross (unpublished).
[27] M. C. Cross (unpublished).
[28] G. Dangelmayr, E. Knobloch, and M. Wegelin, Europhys. Lett. **16**, 8 (1991).
[29] D. Bensimon, B. I. Shraiman, and V. Croquette, Phys. Rev. A **38**, 5461 (1988).